Towards fully automatic mesh generation for Large Eddy Simulation of Turbulent Combustion in a typical micro Gas Turbine Combustor

Antoine Verhaeghe[a], Alessio Pappa[a], Ward De Paepe[a], Pierre Bénard[b], Laurent Bricteux[a]

[a] *Université de Mons, UMONS, Faculté Polytechnique, B7000, Mons, Belgium*
[b] *Université de Normandie, INSA Rouen, UNIROUEN, CNRS, Coria, Rouen 76000 France*

Introduction

Over the last years, several advanced micro Gas Turbine (mGT) cycle developments have been proposed and studied to make the mGT more fuel and operationally flexible. However, accurate data on real industrial combustors, assessing the performances and emissions of the combustion under unconventional diluted conditions or fuels involved in these novel cycles are still missing. In this framework, Large Eddy Simulations (LES), who allow to accurately assess the unsteady effects coupled to turbulent-chemistry interaction of reacting flows, offer an opportunity to better assess the combustion behavior under these specific conditions. However, the computational cost still remains much higher than RANS simulations. Moreover, the mesh generation might be complex, especially when the region of interest is not intuitively known. An innovative solution to simplify mesh generation and to reduce computational cost for an equivalent resolution accuracy lies in dynamic Adaptive Mesh Refinement (AMR). This method allows generating Eulerian elements only in the region where finer cells are required to capture essential effects, i.e. in the flame front. By dynamically refining the mesh all along the simulation, based on a predefined criterion, the mesh is optimized in terms of cell quantity and distribution for more accurate results at potentially lower computational cost [1]. In this work, AMR is applied on the LES of a typical industrial mGT combustor, namely the Turbec T100, to capture combustion more accurately without significantly increasing the computational cost.

Methodology

The mesh adaptation has been applied to the LES performed by Pappa et al. [2] on a simplified geometry of the combustion chamber of the Turbec T100 mGT (Fig. 1), representing the reference case (REF).

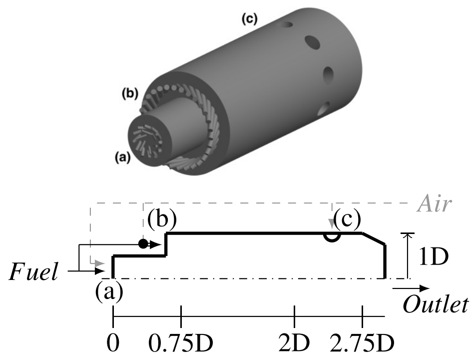

Figure 1: *3D and 2D representations of the simplified geometry of the Turbec T100 mGT combustor where the total combustion air flow rate is distributed as follows: 4 % in the 12 pilot injectors for air (and 6 for fuel) for the diffusion pilot flame (a), 21 % in the 30 main premixed injectors (b) and 75 % through the 9 dilution holes (c).*

Simulations were performed using the massively parallel flow solver YALES2 [3]. The AMR process involves imposing a target metric in regions of interest according to a user-defined criterion. The flame sensor, aiming to identify the flame front for the TFLES model, is used as mesh adaptation criterion. This flame sensor is based on a threshold of a virtual progress variable source term $\dot{\omega}_C$ computed as a products reaction combination $\dot{\omega}_C = \dot{\omega}_{CO_2} + \dot{\omega}_{CO} + \dot{\omega}_{H_2O}$. The flame sensor is set to 1 when $\dot{\omega}_C$ exceeds 10% of its maximal value for a 1D laminar flame in the same operating conditions [4]. The target metric is set to 1 mm, which is the metric used for the REF mesh in the combustion zone. The background mesh is treated in two different ways: a 5 mm constant background metric is imposed for the first case (AMR1), while the initial REF mesh is conserved in background regions for the second case (AMR2). The REF, AMR1 and AMR2 meshes, presented in Fig. 2, are composed of, respectively, 33.1, 19.6 and 34.5 millions of cells. The mesh adaptation triggering is based on the relative metric error, representing the deviation from the target metric:

Email address: antoine.verhaeghe@umons.ac.be

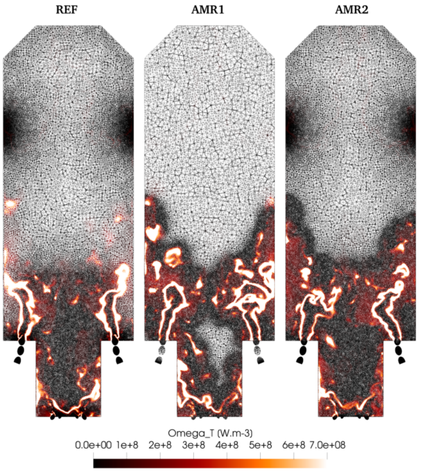

Figure 2: *Comparison of the instantaneous reaction rate fields, superposed to the mesh, in a 2D cross section plan along the axial axis, highlight that in the REF case (left) the flame extends beyond the predefined refined zone, while in both AMR1 (center) and AMR2 (right), the mesh is refined around the flame.*

$$\epsilon = \max\left(\left|\frac{M_{current} - M_{target}}{M_{target}}\right|\right), \quad (1)$$

where $M_{current}$ and M_{target} are respectively the current cell metric and the target cell metric. The AMR is triggered when this relative error exceeds a maximum acceptable error ϵ_{max} set at 200% in this work.

Results

The effect of AMR can be clearly observed in Fig. 2. The mesh refinement follows the flame shape and the flame is well contained in the refined zone at all times. The refined zone is enlarged to ensure a safety margin (7 propagation cells). This safety margin allows compensating metric errors close to 200% while ensuring that the flame is enclosed within the refined mesh.

The mesh adaptation provides a more accurate resolution of combustion in the flame region (Fig. 3). Indeed, slightly higher temperatures are observed close to the wall for both AMR cases compared to the REF case (Z=0.75D). For both AMR cases, the mesh is refined in this region when the flame propagates along the wall, while the REF case presents a coarser mesh in this zone. Therefore, the temperature is more accurately predicted in both AMR cases close to the wall.

However, close to the dilution holes (Z=2D) and at the outlet of the combustion chamber (Z=2.75D), the average and RMS temperature profiles are different for the AMR1 case compared to the REF and AMR2 cases (Fig. 3). Moreover, the average temperature at the outlet are 1244K for the REF case, 1302K for the AMR1 case and 1244K for the AMR2 case. This clearly highlights that the background mesh used for the AMR1 case (constant metric of 5 mm) is too coarse to correctly capture the dilution effect of the flue gas by the cold air, leading to an overestimation of the outlet temperature.

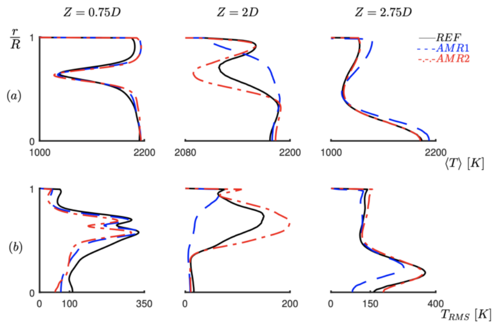

Figure 3: *Comparison of azimuthal time average and RMS temperature (a and b) between the reference (in black), AMR1 (in blue), and AMR2 (in red) cases in 3 positions taken along the combustion chamber: Z=0.75D, Z=2D, and Z=2.75D, demonstrating the benefits of applying AMR in the flame region.*

Regarding the CPU cost, the AMR1 and AMR2 cases are respectively 17% and 70% more expensive than the REF case, highlighting the high cost of dynamic mesh adaptation. Indeed, the mesh adaptation contributes, respectively for the AMR1 and AMR2 cases, to 33% and 15% of the total CPU cost. However, since the REF case provides a less accurate resolution of the combustion, this increase in computational cost remains reasonable.

Conclusion

The AMR strategy based on the flame sensor allows to generate automatically a dynamic mesh that is able to capture correctly the flame over time at a reasonable computational cost. However, this strategy simply based on the flame sensor, does not allow the automatic and correct meshing of the dilution zone at the combustion chamber outlet, which is necessary to predict emissions and flue gas properties precisely. Therefore, to ensure a fully automatic meshing of the combustion chamber to avoid human intervention, an additional adaptation criterion must be considered.

References

[1] P. Bénard, G. Balarac, V. Moureau, C. Dobrzynski, G. Lartigue, Y. D'Angelo, International Journal for Numerical Methods in Fluids 81 (2016) 719–740.

[2] A. Pappa, B. Bricteux, P. Bénard, W. De Paepe, Journal of Engineering for Gas Turbine and Power 143 (2020) 041008.

[3] V. Moureau, P. Domingo, L. Vervisch, Comptes Rendus Mecanique 339 (2-3) (2011) 141–148.

[4] O. Colin, F. Ducros, D. Veynante, T. Poinsot, Physics of Fluids 12 (7) (2000) 1843–1863.